DOI: 10.1002/chem.200802010

Influence of the Charge State on the Structures and Interactions of Vancomycin Antibiotics with Cell-Wall Analogue Peptides: Experimental and Theoretical Studies

Zhibo Yang, Erich R. Vorpagel, and Julia Laskin*[a]

Abstract: In this study we examined the effect of the charge state on the energetics and dynamics of dissociation of the noncovalent complex between the vancomycin and the cell-wall peptide analogue N_α,N_ε-diacetyl-L-Lys-D-Ala-D-Ala (V–Ac_2LKDADA). The binding energies between the vancomycin and the peptide were obtained from the RRKM (Rice, Ramsperger, Kassel, Marcus) modeling of the time- and energy-resolved surface-induced dissociation (SID) experiments. Our results demonstrate that the stability of the complex towards fragmentation increases in the order: doubly protonated < singly protonated < deprotonated. Dissociation of the singly protonated and singly deprotonated complex is characterized by very large entropy effects, which indicate a substantial increase in the conformational flexibility of the resulting products. The experimental threshold energies of (1.75 ± 0.08) eV ((40.3 ± 1.8) kcal mol^{-1}) and (1.34 ± 0.08) eV ((30.9 ± 1.8) kcal mol^{-1}) obtained for the deprotonated and singly protonated complexes, respectively, are in excellent agreement with the results of density functional theory calculations. The increased stability of the deprotonated complex observed experimentally is attributed to the presence of three charged sites in the deprotonated complex, as compared with only one charged site in the singly protonated complex. The low binding energy of (0.93 ± 0.04) eV ((21.4 ± 0.9) kcal mol^{-1}) obtained for the doubly protonated complex suggests that this ion is destabilized by Coulomb repulsion between the singly protonated vancomycin and the singly protonated peptide comprising the complex.

Keywords: binding energy · charge state · density functional calculations · mass spectrometry · noncovalent interactions

Introduction

Noncovalent interactions play an important role in chemistry and biology because they are involved in determining high-order structures and function of biological molecules, molecular recognition, and self-assembly.[1–4] Studies of biomolecular recognition in the gas phase provide important information on the intrinsic properties of noncovalent complexes and the binding energies in the absence of solvent molecules. Consequently, the dissociation of noncovalent complexes is a current research focus in mass spectrometry.[5] The most reliable energetics for these systems have been obtained by using blackbody infrared radiative dissociation (BIRD).[6–8] This method utilizes the photon flux generated by the vacuum chamber walls and the long timescale of a Fourier-transform ion-cyclotron-resonance mass spectrometer (FT-ICR MS) to heat the ions radiatively and to follow their fragmentation as a function of wall temperature. While BIRD provides accurate Arrhenius dissociation parameters, E_a and A, for gas-phase fragmentation of complex ions, our recent study demonstrated that there is a strong correlation between these parameters.[9,10] As a result, the Arrhenius activation energy contains a significant entropic contribution, and therefore does not necessarily reflect the thermochemical stability of the ion. Consequently, accurate determination of threshold energies and activation entropies, two linearly independent parameters, is essential for understanding gas-phase stabilities of noncovalent complexes.

Time- and collision-energy-resolved surface-induced dissociation (SID) combined with RRKM (Rice, Ramsperger, Kassel, Marcus) modeling[11,12] is a powerful approach for studying the energetics and entropy effects of the gas-phase fragmentation of both covalent and noncovalent bonds in

[a] Dr. Z. Yang, Dr. E. R. Vorpagel, Dr. J. Laskin
Chemical and Materials Sciences Division
Pacific Northwest National Laboratory
P.O. Box 999 (K8-88), Richland, WA 99352 (USA)
Fax: (+1) 509-376-6066
E-mail: Julia.Laskin@pnl.gov

Supporting information for this article is available on the WWW under http://dx.doi.org/10.1002/chem.200802010.

large complex ions.[10,13] This approach has been extensively used to explore the energetics and dynamics of the dissociation of even- and odd-electron peptide ions and other complex systems.[10,13–18] Recently, we reported the first determination of the strength of noncovalent binding in a vancomycin–tripeptide complex by using this technique.[19] Vancomycin (V) is a glycopeptide antibiotic that is widely used as a human therapeutic agent. Its antibiotic activity results from its noncovalent interactions with the bacterial cell-wall peptidoglycan terminating in D-Ala-D-Ala (DADA) that inhibits the biosynthesis of the peptidoglycan.[20] The V–DADA interaction is a widely used model system for investigating biomolecular recognition processes and for the development of mass spectrometric approaches for probing the strength of noncovalent interactions.[21–24]

The binding energy of (1.34 ± 0.08) eV ($30.9\,\mathrm{kcal\,mol^{-1}}$) between vancomycin and the peptide ligand was determined from SID data obtained for the singly protonated vancomycin–N_α,N_ε-diacetyl-L-Lys-D-Ala-D-Ala complex (V–Ac_2LKDADA).[19] Gas-phase fragmentation of this complex is dominated by the loss of the neutral peptide. The second minor reaction channel results in the formation of the neutral vancomycin and the singly protonated peptide. RRKM modeling of time- and energy-resolved SID data demonstrated that entropy plays a major role in determining the dissociation rate of the V–Ac_2LKDADA complex. Unusually large values of activation entropies were obtained for both dissociation pathways of this relatively small model system. The corresponding pre-exponential factors of 5.5×10^{30} and $9.4\times10^{26}\,\mathrm{s^{-1}}$ are similar to the values reported for the dissociation of large protein–ligand complexes by using BIRD.[8] The difference in the relative abundances of the two products was attributed to the difference in activation entropies associated with the formation of neutral and protonated peptide fragments. Density functional theory (DFT) calculations performed at the B3LYP/6-31G(d) level of theory provided important insights on the structures and stabilities of different model complexes, and on the contribution of electrostatic and hydrogen-bonding interactions in this model system.[25]

It is well accepted that the structures and the interaction energies of noncovalent complexes in the gas-phase are affected by the charge state of the ion.[26–29] Jørgensen et al. reported a detailed study of gas-phase fragmentation of doubly protonated and doubly deprotonated noncovalent complexes of vancomycin with different peptide ligands by using collisional-induced dissociation (CID) experiments.[30] The results of that study suggested that the original solution-phase structure of vancomycin responsible for selective binding of the D-Ala-D-Ala motif was preserved only in the negative mode. Specifically, they found a good correlation between the relative stabilities of doubly deprotonated complexes toward fragmentation and association constants of these complexes in solution. In contrast, similar fragmentation efficiency curves were obtained for doubly protonated complexes with different peptide ligands, indicating a loss of specific binding between vancomycin and stereoisomers of DAla-DAla-containing peptides in doubly protonated complexes.

Herein, we present a comparison of the dependence of the relative stability of the V–Ac_2LKDADA complex on the charge state of the ion by comparing the energetics and dynamics of dissociation of the singly protonated, doubly protonated, and singly deprotonated complex. The experimental binding energies are compared with theoretical values obtained by using DFT. Comparison between experiment and theory provides important information about possible structures of the V–Ac_2LKDADA complex in the gas phase. The results demonstrate that the charge state of the complex has a significant effect on its structure and stability towards fragmentation.

Results and Discussion

SID of the singly protonated V–Ac_2LKDADA complex was discussed in detail in our previous study.[19] Fragmentation of the $[V+Ac_2LKDADA+H]^+$ ion (Scheme 1) results in the

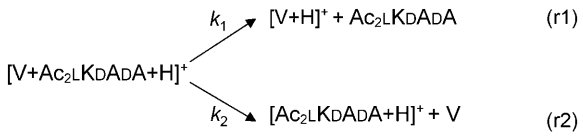

Scheme 1.

formation of the protonated vancomycin, $[V+H]^+$, as a major fragment together with a minor product that corresponds to the singly protonated Ac_2LKDADA. Fragmentation of the doubly protonated complex, summarized in Scheme 2, is dominated by the formation of the two complementary singly protonated fragment ions, $[V+H]^+$ and $[Ac_2LKDADA+H]^+$. Typical SID spectra of the deprotonated complex are shown in Figure 1. $[V-H-CO_2]^-$ is a major fragment of the deprotonated complex at all collision energies. Minor fragments include the $[V-H]^-$ ion observed at very low abundance ($<3\%$) in the range of collision energies between 36 and 48 eV and the deprotonated peptide, $[Ac_2LKDADA-H]^-$, formed at collision energies above 36 eV. In addition, consecutive fragmentation of the $[V-H-CO_2]^-$ results in the formation of minor $[V-H-CO_2-301]^-$ and $[V-H-CO_2-929]^-$ fragment ions at collision energies above 72 eV.

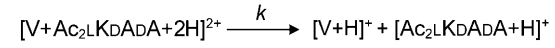

Scheme 2.

Time-resolved survival curves (SCs) of the precursor ion and fragmentation efficiency curves (TFECs) for the fragments were obtained by varying the collision energy and the reaction time, and then by plotting the relative abundance

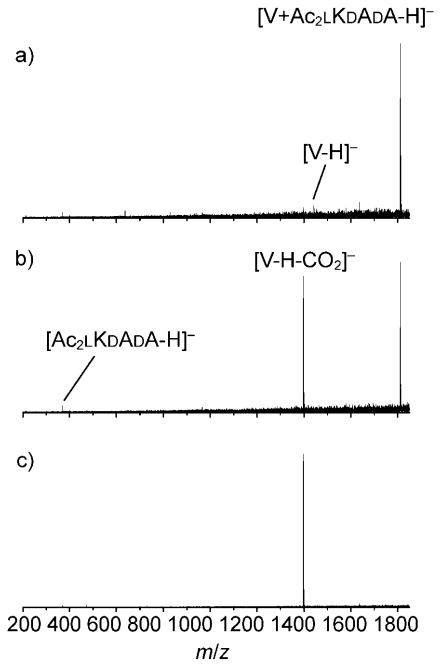

Figure 1. SID spectra of $[V+Ac_2LKDADA-H]^-$ complexes at collision energies of a) 40.5 eV, b) 58.5 eV, and c) 78.5 eV at reaction delays of 1 ms.

of each ion as a function of collision energy for each fragmentation delay. The relative abundance of the precursor ion and its fragments was determined by summation of the corresponding isotopic peaks. Careful examination of the collision-energy-resolved data suggests that the formation of the $[V-H]^-$ ion is the lowest-energy-dissociation pathway of the deprotonated complex, which has an appearance energy of approximately 35 eV. TFECs are obtained for this fragment peak at 40–45 eV and decrease to zero at approximately 55 eV. Rapid decrease in the relative abundance of the $[V-H]^-$ fragment is accompanied by formation of the abundant $[V-H-CO_2]^-$ ion, suggesting that this fragment is most likely produced by subsequent fragmentation of the relatively unstable $[V-H]^-$ primary fragment ion. The proposed fragmentation pathways for the deprotonated complex are summarized in Scheme 3. Abundant formation of the $[V-H-CO_2]^-$ ion has been previously observed in CID of the doubly deprotonated V–Ac_2LKDADA complex.[30b] This product ion was attributed to the sequential loss of CO_2 from the primary $[V-H]^-$ fragment.

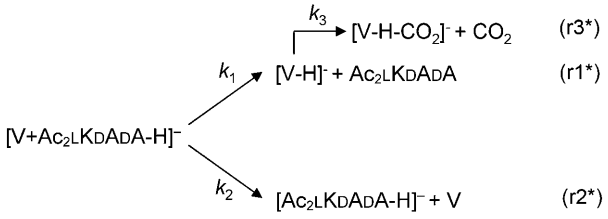

Scheme 3.

The relative stability of the V–Ac_2LKDADA complex towards fragmentation is a strong function of its charge state. Figure 2 compares SCs of the $[V+Ac_2LKDADA+H]^+$, $[V+Ac_2LKDADA+H]^{+2}$, and $[V+Ac_2LKDADA-H]^-$ ions obtained at reaction delays of 1 and 50 ms. The collision energy required for the dissociation of different charge states of the complex increases in the order $[V+Ac_2LKDADA+2H]^{2+} < [V+Ac_2LKDADA+H]^+ < [V+Ac_2LKDADA-H]^-$, suggesting that both positively charged complexes are much less stable toward fragmentation than the deprotonated complex. The experimental SCs shown in Figure 2 exhibit fairly weak dependence on the reaction time, which indicates a very loose transition state associated with the decomposition of the complexes. For example, increasing the reaction delay from 1 to 50 ms results in a 4.7 eV decrease (from 58.5 to 53.8 eV) in collision energy required to reach the point at which 50% of the $[V+Ac_2LKDADA-H]^-$ ion has decomposed ($E_{50\%}$). The corresponding shifts of 4.2 and 7.4 eV were observed for the $[V+Ac_2LKDADA+H]^{+2}$ and $[V+Ac_2LKDADA+H]^+$ complexes, respectively.

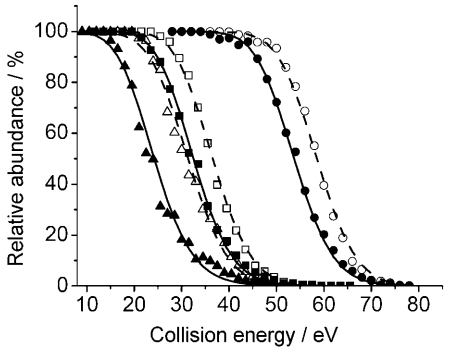

Figure 2. Experimental SCs for the precursor ion of the singly protonated (□, ■), doubly protonated (△, ▲), and singly deprotonated (○, ●) V–Ac_2LKDADA complexes obtained at reaction delays of 1 ms (open symbols) and 50 ms (filled symbols). The lines correspond to the best fits obtained from the RRKM modeling of the 1 ms (-----) and 50 ms (——) data.

The solid lines shown in Figure 2 correspond to the best fit obtained from the RRKM modeling,[11,12] described in detail in the Supporting Information. Breakdown graphs for dissociation of the $[V+Ac_2LKDADA+2H]^{2+}$ and $[V+Ac_2LKDADA-H]^-$ ions were constructed based on the fragmentation pathways shown in Schemes 2 and 3. Specifically, dissociation of the $[V+Ac_2LKDADA+2H]^{2+}$ ion was modeled by using a single decay rate, whereas the three decay rate model was used for the deprotonated complex. Radiative cooling of the precursor ion was taken into account in all models. Modeling results for the doubly protonated complex were obtained by fitting the SCs of the precursor ion, whereas dissociation parameters for the deprotonated complex were obtained from the simultaneous fitting of the SCs of the precursor ion and TFECs obtained for the $[V-H]^-$, $[V-H-CO_2]^-$, and $[Ac_2LKDADA-H]^-$ fragment

ions. The relative abundance of the $[V-H-CO_2]^-$ ion used in the modeling included the abundances of its subsequent fragments, $[V-H-CO_2-301]^-$ and $[V-H-CO_2-929]^-$, observed at higher collision energies.

Figure 3 shows the best fit of the experimental data obtained for the deprotonated complex. The agreement between the experiment and the model is fairly good, particularly for the precursor ion and the major $[V-H-CO_2]^-$ fragment. The model also provides a reasonable representation of the major trends in the experimental TFECs for the primary $[V-H]^-$ and $[Ac_2LKDADA-H]^-$ fragment ions. However, because of the low abundance of these species and the significant scatter of the experimental data points, the agreement between the experiment and model is not as good. It should be noted that the only model that adequately describes the TFECs of the $[Ac_2LKDADA-H]^-$ fragment ion is based on the assumption that the initial structures of the $[V+Ac_2LKDADA-H]^-$ complexes that decompose through reactions r1* and r2* are different. We found that only a small fraction of precursor complexes (ca. 0.8%) are responsible for the formation of the $[Ac_2LKDADA-H]^-$ product ion, whereas the rest of the ions undergo fragmentation through reaction r1*. It follows that loss of the deprotonated peptide does not directly compete with the loss of the neutral peptide from the complex.

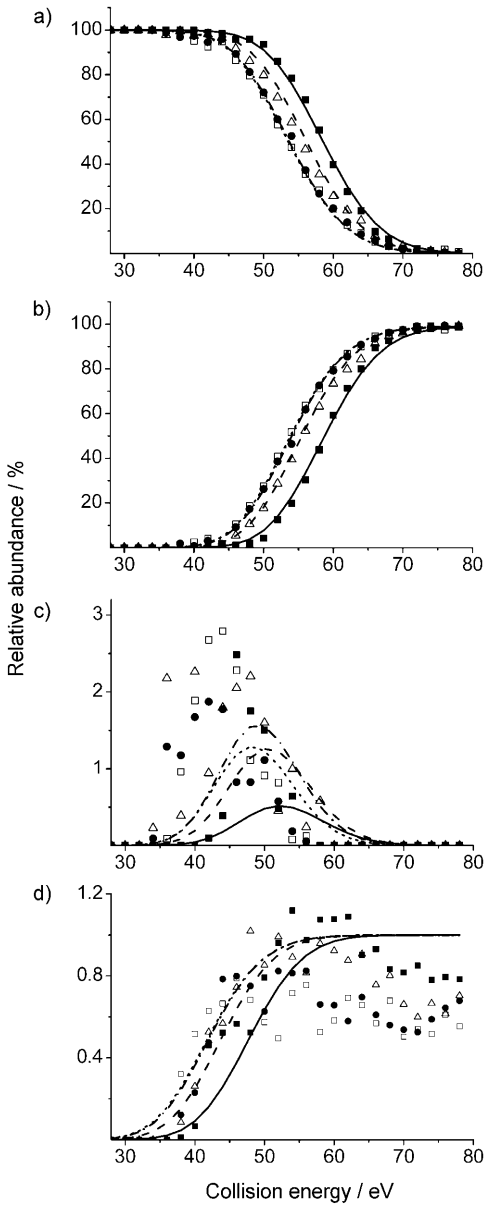

Figure 3. RRKM modeling fit (lines) of the experimental data (symbols) for a) the decomposition of $[V+Ac_2LKDADA-H]^-$, b) the major $[V-H-CO_2]^-$ fragment, c) the minor $[V-H]^-$ fragment, and d) the minor $[Ac_2LKDADA-H]^-$ fragment for reaction delays of 1 (■, ——), 10 (△, -----), 50 (●, –•–•), and 100 ms (□, -----).

Dissociation parameters obtained for all three charge states of the complex are summarized in Table 1. The large uncertainties in the values of dissociation parameters obtained for the minor dissociation channel of the deprotonated complex originate from the significant scatter in the TFECs of the $[Ac_2LKDADA-H]^-$ fragment ion. Loss of the neutral peptide from the singly protonated and singly deprotonated complexes is characterized by similar activation entropies and very different threshold energies of 1.34 and 1.75 eV (30.9 and 40.3 kcal mol^{-1}), respectively. Very large entropy effects indicate a substantial increase in the conformational flexibility of the resulting products. Because entropy effects for reactions r1 and r1* are the same within the experimental uncertainty, we conclude that the lower stability of the protonated complex results from weaker interaction between the positively charged vancomycin cage and the neutral peptide ligand. In contrast, both the threshold energy and the activation entropy for dissociation of the doubly protonated complex are much lower than the dissociation parameters obtained for the singly charged ions. Addition of the second proton results in a decrease of approximately 0.4 eV (9.2 kcal mol^{-1}) in the binding energy of the positively charged complex and 11–13 orders of magnitude decrease in the pre-exponential factor. It follows that al-

Table 1. Threshold energies and activation entropies for the dissociation channels of different charge states of the V–$Ac_2LKDADA$ complex obtained from the RRKM modeling of the time- and collision-energy-resolved SID data. Rate constants k_1 and k_2 are defined in Schemes 1–3.

Systems	Parameters	k_1	k_2
$[V+Ac_2LKDADA+H]^+$	E_0 [eV]	1.34 ± 0.08	1.32 ± 0.08
	$\Delta S^{\neq[a]}$ [e.u.]	79 ± 4	62 ± 4
	$A^{[b]}$ [s^{-1}]	6×10^{30}	9×10^{26}
$[V+Ac_2LKDADA+2H]^{2+}$	E_0 [eV]	0.93 ± 0.04	–
	$\Delta S^{\neq[a]}$ [e.u.]	27 ± 7	–
	$A^{[b]}$ [s^{-1}]	2×10^{19}	–
$[V+Ac_2LKDADA-H]^-$	E_0 [eV]	1.75 ± 0.08	1.56 ± 0.40
	$\Delta S^{\neq[a]}$ [e.u.]	87 ± 7	89 ± 53
	$A^{[b]}$ [s^{-1}]	6×10^{32}	6×10^{32}

[a] Entropy units (e.u.) = cal mol^{-1}K^{-1}. [b] Calculated from $\Delta S^{\neq}$ by assuming a temperature of 450 K.

though fragmentation of the $[V+Ac_2LKDADA+2H]^{2+}$ ion is energetically favorable, it is kinetically more hindered than dissociation of the singly charged complex. This result is reasonable because fragmentation of a doubly charged ion is always associated with a substantial Coulomb barrier for the reverse reaction.

Structures of V–Ac_2LKDADA complexes: DFT calculations were performed to examine possible structures of the deprotonated V–Ac_2LKDADA complex. The corresponding calculations for the singly protonated complex were presented in our previous study.[19] Because loss of a neutral peptide ligand is characterized by a very loose transition state, the energetics of this reaction can be adequately described by using calculated energies of the corresponding products, Ac_2LKDADA and $[V-H]^-$.

The deprotonated V–Ac_2LKDADA complex can be composed of a neutral peptide and a deprotonated cage, or a vancomycin with a net zero charge (zwitterionic or canonical) and a deprotonated peptide ligand. Relative energies of different possible structures of the deprotonated complex are summarized in Table 2. Molecular dynamics (MD; values reported in kcal mol^{-1} only) simulations performed by using the CFF91 force field suggest that the most stable structure of the $[V+Ac_2LKDADA-H]^-$ complex is composed of the deprotonated peptide and the zwitterionic vancomycin cage, in which the C terminus is deprotonated and the primary amine of the disaccharide (N_a) is protonated (model system $[VZW1][Ac_2LKDADA-H]^-$). Other possible structures examined by using MD simulations include the zwitterionic structure, in which the C terminus of vancomycin is deprotonated and the secondary amine of the *N*-methylleucine is protonated, $[VZW2][Ac_2LKDADA-H]^-$; the canonical structure composed of the deprotonated peptide and the neutral vancomycin, $[V][Ac_2LKDADA-H]^-$; and the canonical structure composed of the deprotonated vancomycin and the neutral peptide, $[V-H]^-[Ac_2LKDADA]$. These structures are 52.8, 87.7, and 99.4 kcal mol^{-1}, respectively, less stable than the lowest-energy zwitterionic structure. Even though the absolute energetics obtained from MD simulations is not accurate, the trend in the relative stability is qualitatively correct. A similar trend in relative stabilities of the deprotonated $[VZW1][Ac_2LKDADA-H]^-$, $[VZW2][Ac_2LKDADA-H]^-$, and $[V][Ac_2LKDADA-H]^-$ complexes was obtained by using DFT optimization performed at the B3LYP/3-21G level of theory. DFT calculations indicate that $[VZW1][Ac_2LKDADA-H]^-$ is the most stable structure, whereas $[VZW2][Ac_2LKDADA-H]^-$ and $[V][Ac_2LKDADA-H]^-$ are less stable than $[VZW1][Ac_2LKDADA-H]^-$ by 16.0 and 36.8 kcal mol^{-1}, respectively.

Table 2. Relative energies of the lowest-energy structures of $[V+Ac_2LKDADA-H]^-$ model complexes obtained from MD simulations and DFT calculations [kcal mol^{-1}].

Complex	Model systems[a]	MD	DFT[b]
$[V+Ac_2LKDADA-H]^-$	$[V-H]^-[Ac_2LKDADA]$	99.4	–
	$[V][Ac_2LKDADA-H]^-$	87.7	36.8
	$[VZW1][Ac_2LKDADA-H]^-$	0.0	0.0
	$[VZW2][Ac_2LKDADA-H]^-$	52.8	16.0

[a] Model systems are described in the text. [b] Obtained from geometry optimization performed at the B3LYP/3-21G level of theory.

Because of limited computational resources, only the lowest-energy structure of the $[V+Ac_2LKDADA-H]^-$ model complex, $[VZW1][Ac_2LKDADA-H]^-$, was selected for subsequent optimization by using ONIOM(B3LYP/6-31G(d):B3LYP/3-21G) calculations. In the optimized structure of the complex shown in Figure 4, the protonated N_a of vancomycin and the deprotonated C termini of the vancomycin and the peptide are involved in the intermolecular hydrogen bonding in the complex. The protonated N_a is solvated by the carbonyl groups of V and $[Ac_2LKDADA-H]^-$ and the carboxylate group of $[Ac_2LKDADA-H]^-$ through three strong hydrogen bonds (1.71–2.26 Å). The carboxylate group of the vancomycin is stabilized by three amide groups of the peptide through four hydrogen bonds (1.85–2.46 Å), and the carboxylate group of $[Ac_2LKDADA-H]^-$ forms strong hydrogen bonds (1.89–2.42 Å) with four amide groups of the vancomycin and the secondary amine of *N*-methylleucine. In addition, two hydroxyl groups of the disaccharide moiety and one of the substituted phenylglycines, as well as one primary amine group of the *N*-methylleucine of vancomycin, form three strong hydrogen bonds (1.78–1.97 Å) with three carbonyl groups of the peptide.

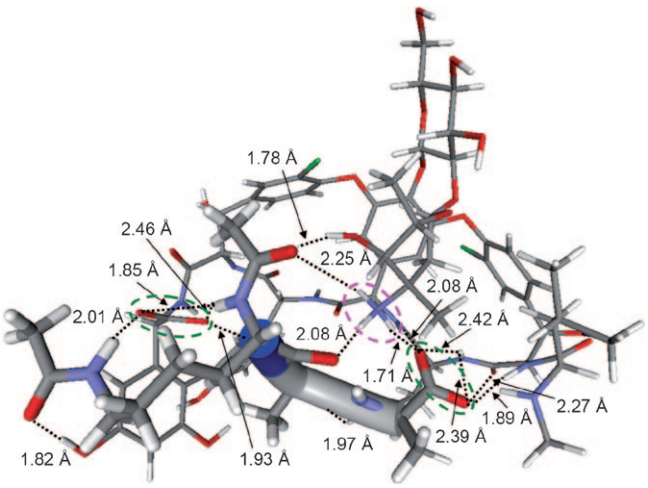

Figure 4. Lowest-energy structure of the deprotonated V–Ac_2LKDADA complex, $[VZW1][Ac_2LKDADA-H]^-$, obtained by using the ONIOM-(B3LYP/6-31G(d):B3LYP/3-21G) method. Vancomycin is shown with thin lines, whereas the Ac_2LKDADA peptide is shown with thick lines with the backbone shown as colored tubes; the dotted lines indicate the intermolecular hydrogen bonds between the vancomycin and Ac_2LKDADA. -----: protonation site. -----: deprotonated carboxyl groups of the peptide and vancomycin.

Comparison of the structures of the protonated[19] and the deprotonated V–Ac_2LKDADA complex indicates that, for both charge states, the protonated disaccharide group is folded into the vancomycin cage and is involved in the inter-

molecular hydrogen bonding. However, deprotonation of the C-terminal carboxyl groups of both vancomycin and peptide in the negatively charged complex results in the formation of a number of additional strong hydrogen bonds, which stabilize the charges. It is likely that these interactions are responsible for the higher binding energy between the peptide ligand and the cage in the deprotonated V–Ac_2LKDADA complex determined from our SID experiments.

It is interesting to note some similarities between the calculated structure of the deprotonated complex and the structure of V–Ac_2LKDADA in solution.[3,22,31] In both cases, the deprotonated C termini of the peptide and vancomycin are involved in the intermolecular hydrogen bonding. The interaction between the deprotonated C terminus of the peptide with the *N*-methylleucine group (2.1 Å) is preserved in the gas phase. It has been suggested that the electrostatic interaction between these two groups contributes 1.4–1.8 kcal mol^{-1} to the binding energy of the V–Ac_2LKDADA complex in solution.[31b] The major difference between the solution and gas-phase structures is that in solution the protonated disaccharide group of vancomycin is stabilized by interactions with solvent molecules and is not involved in the intermolecular hydrogen bonding, whereas in the gas phase this group is stabilized through a strong electrostatic interaction with the deprotonated C terminus of the peptide.

Binding energies: As discussed in our previous study, conformational flexibility of the reaction products introduces a significant uncertainty into the calculated values of the binding energies. In particular, it is not clear whether the conformational change in the products occurs in the transition state or after they separate from each other. The lower and upper limits of the binding energies were obtained from the energies of the lowest-energy structures of the products at infinite separation, and the energies of less stable structures that resemble the conformations of the peptide and vancomycin in the complex. It should be noted that the DFT energetics obtained for the negative complex may not be very accurate because the basis sets utilized in this study do not include diffuse functions. However, we believe that the uncertainty in the binding-energy calculations introduced because of the conformational flexibility of the reaction products is substantially more significant than the uncertainty introduced by the limitations of the basis sets.

The lowest-energy conformation of the neutral peptide (Figure S1a in the Supporting Information) was adopted from our previous study. The second conformation representing the structure of the neutral peptide in the transition state optimized at the B3LYP/6-31G(d) level of theory (Figure S1b in the Supporting Information) is only 3.0 kcal mol^{-1} higher in energy. In contrast, the lowest-energy structure of deprotonated vancomycin (Figure S2a in the Supporting Information) is 18.8 kcal mol^{-1} more stable than the extended conformation adopted by the cage in the complex (Figure S2b in the Supporting Information). The folded conformation (Figure S2a in the Supporting Information) was initially adopted from the lowest-energy structure obtained by using MD simulations, and then optimized by using the ONIOM (B3LYP/6-31G(d):B3LYP/3-21G) method, whereas the extended conformation (Figure S2b in the Supporting Information) was initially obtained from the most stable structure of the $[V+Ac_2LKDADA-H]^-$ species and optimized by using the same method.

In the folded conformation, the neutral disaccharide group resides outside of the vancomycin cage. The asparagine side chain is folded into the vancomycin cage and forms four hydrogen bonds (2.20–2.92 Å) with the carbonyl and secondary amine groups of the vancomycin cage. In addition, the deprotonated C terminus is stabilized by two short hydrogen bonds (1.34 and 1.93 Å) formed between the adjacent secondary amine and the hydroxyl group of one of the adjacent substituted phenylglycines. In contrast, in the extended conformation, the neutral disaccharide group is folded into the vancomycin cage and forms one hydrogen bond (2.37 Å) with a carbonyl group of the vancomycin cage. The vancomycin cage in this conformation is more open because the deprotonated C terminus is not involved in the hydrogen-bonding interaction with the vancomycin cage.

Calculated values of the binding energies of the vancomycin–peptide complex obtained from the difference in the energy of the reactant and the major products are summarized in Table 3. Because of the large uncertainty in the energy of the $[V-H]^-$ ion, the difference between the upper and lower limit of the theoretical binding energy between the deprotonated vancomycin and the neutral peptide is very large (ca. 22 kcal mol^{-1}). The calculated binding energy is in the range of 40.9–62.7 kcal mol^{-1}. In comparison, the experimental result obtained for the neutral peptide loss from the deprotonated complex (reaction r1*) is (42.7 ± 1.8) kcal mol^{-1}. The experimental value is in excellent agreement with the lower limit of the calculated binding energy of 40.9 kcal mol^{-1}. This comparison suggests that the struc-

Table 3. Comparison of the binding energies of different charge states of the V–Ac_2LKDADA complex obtained experimentally and from the DFT calculations [kcal mol^{-1}].

Complex	Theory			Experiment
	Model system	$E^{[a]}$	$E_0{}^{[a,b]}$	$k_1{}^{[c]}$
$[V+Ac_2LKDADA+H]^{+[d]}$	$[V+H]^+[Ac_2LKDADA]$	46.7 (40.7)	42.0 (36.3)	30.9 (±1.8)
$[V+Ac_2LKDADA+2H]^{2+}$	$[V+2H]^{2+}$ $[Ac_2LKDADA]$	51.7 (47.2)	–	21.4 (±0.9)
$[V+Ac_2LKDADA-H]^-$	$[VZW1][Ac_2LKDADA-H]^-$	69.5 (49.1)	62.7 (40.9)	40.3 (±1.8)

[a] Upper and lower limits (values in parentheses) of the binding energies obtained from the geometry optimization and single point energy calculation by using the ONIOM(B3LYP/6-31G(d):B3LYP/3-21G) method. [b] Including the ZPE correction obtained at the B3LYP/3-21G level of theory. [c] Obtained from the RRKM modeling of the experimental data. [d] Adopted from ref. [19].

tures of the $[V-H]^-$ ion and the neutral peptide in the transition state resemble the lowest-energy folded conformations of the products. A similar result was obtained for the protonated V–Ac_2LKDADA complex.[19]

As discussed earlier, the threshold energy for dissociation of the doubly protonated V–Ac_2LKDADA complex is approximately 0.4 eV (9.2 kcal mol^{-1}) lower than the threshold energy for the loss of the neutral peptide from the singly protonated complex, suggesting that the second proton has a strong destabilizing effect on the V–Ac_2LKDADA complex. In addition, the major dissociation channels for the two positively charged complexes are very different. Specifically, formation of the two complementary singly protonated products is the major fragmentation pathway of the $[V+Ac_2LKDADA+2H]^{2+}$ ion, whereas fragmentation of the $[V+Ac_2LKDADA+H]^+$ ion is dominated by the loss of the neutral peptide. These observations are consistent with the trend in the proton affinities (PAs) of the vancomycin and the peptide.

We have previously shown that the most stable structure of vancomycin is protonated at the disaccharide group. The calculated PA of vancomycin is 272.1 kcal mol^{-1} without the zero-point energy (ZPE) correction and 254.4 kcal mol^{-1} when including the ZPE correction.[19] The corresponding values of 237.6 and 229.2 kcal mol^{-1} were obtained for Ac_2LKDADA, which is protonated at the secondary amine of the acetylated lysine side chain. The second PA of vancomycin obtained in this study by using the ONIOM(B3LYP/6-31G(d):B3LYP/3-21G calculation is 230.9 kcal mol^{-1} without the ZPE correction. This value is lower than the PA of the peptide, suggesting that charge separation in dissociation of the doubly protonated complex is energetically more favorable than the loss of the neutral peptide. It is also reasonable to assume that the $[V+Ac_2LKDADA+2H]^{2+}$ ion is composed of the singly protonated vancomycin and singly protonated peptide ligand. However, because complexation affects the conformational flexibility of the peptide, the PA of the peptide bound to the vancomycin cage may be substantially reduced.

Because the CFF91[32] force field did not include parameters for the protonated amide ($CONH_2^+$) in the Insight II software package used in this study, we could only perform MD simulations for the doubly protonated complex with both protons located on vancomycin. The lowest-energy structure obtained for this complex from MD simulations was subsequently optimized by using ONIOM(B3LYP/6-31G(d):B3LYP/3-21G) calculations. The theoretical binding energy without the ZPE correction obtained at this level of theory is 47.2–51.7 kcal mol^{-1} (Table 3). Because ZPE corrections for the binding energies obtained for the singly protonated[19] and deprotonated V–Ac_2LKDADA complexes are 4.4–4.7 and 6.8–8.2 kcal mol^{-1}, respectively, we assumed that the ZPE correction for the doubly protonated V–Ac_2LKDADA complex does not exceed 10 kcal mol^{-1}. It follows that the theoretical binding energy with ZPE correction obtained for this model system cannot be lower than 37 kcal mol^{-1}. It should be noted that because of the Coulomb repulsion between the products in the transition state, the actual threshold energy for the charge separation reaction is higher than the reaction endothermicity that was calculated based on the enthalpies of formation of the reactant and the products. The value of the binding energy estimated for the V–Ac_2LKDADA complex with both protons residing on vancomycin is clearly inconsistent with the experimentally determined threshold energy of (21.4 ± 0.9) kcal mol^{-1} (Table 3). From the discussion above it follows that the doubly protonated V–Ac_2LKDADA complex examined in our experiments is less stable than the model system used in our DFT calculations. It is reasonable to assume that the complex is composed of the singly protonated vancomycin and the singly protonated peptide ligand, and that its stability is reduced because of the electrostatic repulsion between the charges.

Finally, it is interesting to discuss the energetics of the CO_2 loss from the deprotonated vancomycin. As mentioned earlier, loss of CO_2, a dominant decomposition pathway of the deprotonated vancomycin, is not observed for the deprotonated V–Ac_2LKDADA complex. DFT calculations were performed for the substituted phenylglycine (*N*-methoxyl-2-methyl-3,5-dihydroxylphenylglycine, Figure 5), which represents a small portion of the $[V-H]^-$ with the deprotonated C terminus. A relaxed potential-energy scan performed at the B3LYP/6-31G(d) level of theory indicates that the CO_2 elimination reaction of the model anion proceeds through a loose transition state by C–C bond cleavage at the deprotonated C terminus. The bond energy of 28.8 kcal mol^{-1} obtained for this model system at the B3LYP/6-311++G(2d,2p)//B3LYP/6-31G(d) level of theory is significantly lower than the experimental binding energy of the deprotonated complex ((42.6 ± 1.8) kcal mol^{-1}), suggesting that elimination of CO_2 should be a dominant process for the de-

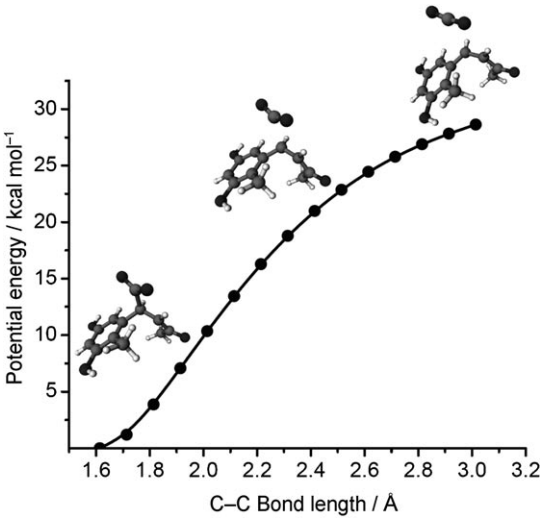

Figure 5. Relaxed potential-energy scan for CO_2 elimination from the deprotonated *N*-methoxyl-2-methyl-3,5-dihydroxylphenylglycine performed at the B3LYP/6-31G(d) level of theory.

protonated vancomycin cage. Suppression of this dissociation channel most likely indicates the involvement of the deprotonated C terminus in the hydrogen bonding. This conclusion is supported by the DFT calculations of the structures of the $[V+Ac_2LKDADA-H]^-$ and the $[V-H]^-$ ions. Indeed, the deprotonated carboxylate group in the $[V+Ac_2LKDADA-H]^-$ complex shown in Figure 4 is stabilized by four strong hydrogen bonds (1.85–2.46 Å), whereas the carboxylate group of the deprotonated vancomycin is involved in only two hydrogen bonds (1.34 and 1.93 Å) in the folded $[V-H]^-$ structure (Figure S1b in the Supporting Information). Elimination of the neutral peptide from the $[V+Ac_2LKDADA-H]^-$ complex disrupts the hydrogen bonding that constrains the $-COO^-$ group, making the loss of CO_2 kinetically favorable.

Conclusion

In this study we used time- and collision-energy-resolved SID experiments combined with RRKM modeling to examine the effect of the charge state on the stability of the V–Ac_2LKDADA complex toward fragmentation. We found that even though the entropy effects in the dissociation of the singly protonated and singly deprotonated complex are very similar, dissociation of the positive ion is energetically more favorable and the deprotonated complex is approximately 0.4 eV (9.2 kcal mol^{-1}) more stable toward fragmentation. The increased stability of the deprotonated complex observed experimentally is consistent with the results of DFT calculations. The experimental threshold energy of (1.75 ± 0.08) eV ((40.3 ± 1.8) kcal mol^{-1}) is in excellent agreement with the lower limit of the calculated binding energy of 40.9 kcal mol^{-1} obtained from the absolute energies of the fragments in their most stable conformation, suggesting that the transition state for dissociation of the complex is located close to the reaction products. Similarly, the experimental threshold energy for dissociation of the singly protonated complex of (1.34 ± 0.08) eV ((30.9 ± 1.8) kcal mol^{-1}) is in good agreement with the lower-limit value of 36.3 kcal mol^{-1} obtained from DFT calculations. Comparison between the calculated lowest-energy structures of the $[V+Ac_2LKDADA+H]^+$ and $[V+Ac_2LKDADA-H]^-$ ions suggests that additional stabilization of the deprotonated complex results from extensive solvation of three charged sites (protonated disaccharide amino group and deprotonated C termini of the vancomycin and the peptide) as compared with only one charged site (protonated disaccharide amino group) in the $[V+Ac_2LKDADA+H]^+$ ion.

Dissociation of the doubly protonated complex is dominated by charge separation of the two singly protonated $[V+H]^+$ and $[Ac_2LKDADA+H]^+$ fragment ions. This reaction is characterized by a fairly low dissociation threshold of (0.93 ± 0.04) eV ((21.4 ± 0.9) kcal mol^{-1}) and a much lower pre-exponential factor of 2×10^{19} s^{-1} than 6×10^{32} s^{-1} obtained for the singly charged complex. While full comparison with DFT calculations could not be performed for this complex, we found that the lowest-energy structure of the doubly protonated complex composed of the doubly protonated vancomycin and the neutral peptide was not formed in our experiments. The high binding energy of >37 kcal mol^{-1} obtained for this structure is comparable to the theoretical binding energy of the singly protonated complex, suggesting that the Coulomb repulsion between the two protons on the vancomycin cage is compensated by stronger hydrogen-bonding interactions around the two charge sites. In contrast, the $[V+Ac_2LKDADA+2H]^{2+}$ ion examined experimentally is substantially less stable toward fragmentation than the $[V+Ac_2LKDADA+H]^+$ ion. It is reasonable to assume that the less stable, doubly protonated complex produced in the electrospray source of our instrument is composed of the singly protonated vancomycin and the singly protonated peptide ligand. Fragmentation behavior of the complex provides further support for this conclusion.

Comparison between the experimental data and the results of DFT calculations provides an important insight into the possible structures of noncovalent complexes and the origin of the differences in binding energies obtained from our time- and collision-energy-resolved SID studies.

Experimental Section

Materials: Self-assembled monolayers (SAMs) were prepared on a single gold {111} crystal (Monocrystals, Richmond Heights, OH) by using a standard procedure. Prior to SAM deposition, the gold surface was cleaned by using a UV cleaner (Boekel Industries, model 135500) for 10 min, and then immersed for at least 12 h in a 1 mM solution of 1-dodecanethiol in ethanol, (Sigma–Aldrich, St. Louis, MO). Extra layers of the SAMs were removed by ultrasonic cleaning in ethanol for 10 min prior to the experiments. Vancomycin hydrochloride and Ac_2LKDADA were purchased from Sigma–Aldrich. The samples were dissolved in a methanol/water (50:50 v/v) solution to a final concentration of vancomycin/Ac_2LKDADA of 300:50 (μM/μM) for the positive mode experiments, and in a methanol/acetonitrile/water (45:45:10 v/v/v) solution to a final concentration of vancomycin/Ac_2LKDADA of 50:50 (μM/μM) for the negative-mode experiments. A syringe pump (Cole Parner, Vernon Hills, IL) was used for direct infusion of the electrospray sample at a flow rate of 25–40 μL h^{-1}.

Mass spectrometry: SID experiments were conducted by using a specially fabricated 6T FT-ICR mass spectrometer described in detail elsewhere.[33] The instrument was equipped with an external electrospray ionization source consisting of an ion funnel[34] followed by three quadrupoles. Ions exiting the ion funnel undergo collisional relaxation and focusing in the first radio-frequency-only collisional quadrupole prior to transfer into a commercial Extrel quadrupole mass filter. Mass selected ions were efficiently thermalized in the accumulation quadrupole, which removed internal and translational energy originating from the ion source and the ion funnel. After accumulation, ions were extracted from the third quadrupole and transferred into the ICR cell where they collided with the surface positioned at the rear trapping plate of the cell. Scattered ions were captured by raising the potentials on the front and rear trapping plates of the ICR cell by 10–20 V. Immediately following the reaction delay, ions were excited by a broadband chirp and detected. The collision energy was defined by the difference between the d.c. offset of the accumulation quadrupole and the potential applied to the rear trapping plate of the ICR cell and the SID target. Data acquisition was accomplished with a MIDAS data station.[35] Time-resolved spectra were obtained by varying the delay between the gated trapping of ions in the ICR cell and the excitation/detection event (the reaction delay). Experiments were performed

for reaction delay times of 1, 5, 10, 50, and 100 ms, and 1 s. TFECs were constructed from experimental mass spectra by plotting the relative abundance of the precursor ion and its fragments as a function of collision energy for each reaction delay.

MD simulations: Molecular modeling was performed on an SGI Onyx 3200 workstation running Insight II/Discover (97.0, Accelrys Software, San Diego, CA) software. The original structure of vancomycin was obtained from the protein data bank (PDB) and was used as the reference.[36] Preliminary structures of the neutral and deprotonated species of peptide (Ac_2LKDADA and [Ac_2LKDADA−H]$^-$), vancomycin (V and [V-H]$^-$), and the singly deprotonated vancomycin–peptide model complexes ([V][Ac_2LKDADA−H]$^-$ and [V−H]$^-$[Ac_2LKDADA]) were built by using the Biopolymer builder of Insight II. Both initial and final structures were energy minimized with the CFF91 force field[32] and the quasi-Newton–Raphson (VA09 A) minimization algorithm.[37] Conformational space of the complex ions and neutral molecules was explored by using MD simulations performed at 1000 K for monomers (V, [V−H]$^-$, Ac_2LKDADA and [Ac_2LKDADA−H]$^-$) and 500 K for complexes ([V][Ac_2LKDADA−H]$^-$ and [V−H]$^-$[Ac_2LKDADA]) in vacuum with a 1.0 fs time step. Conformations were saved at 2 ps intervals over a 1 ns dynamics run. Each structure was then minimized and the lowest-energy structure of each species was chosen for DFT calculations.

DFT calculations: DFT calculations were carried out by using NWChem (version 5.1), developed and distributed by the Pacific Northwest National Laboratory (PNNL).[38] Extensible Computational Chemistry Environment (ECCE) was used to setup calculations and visualize the results.[39] Preliminary geometry optimization was performed at the B3LYP/3-21G level of theory. Final geometries and single-point energies of Ac_2LKDADA and [Ac_2LKDADA−H]$^-$ were obtained by subsequent optimization at the B3LYP/6-31G(d) level of theory. The hybrid computational method (ONIOM) was used for the structure optimizations and single-point energy calculations for [V−H]$^-$ and [VZW1][Ac_2LKDADA−H]$^-$, in which B3LYP/6-31G(d) was applied to Ac_2LKDADA and the atoms related to the hydrogen bonding between vancomycin and the peptide in the [VZW1][Ac_2LKDADA−H]$^-$ model complex, and B3LYP/3-21G was applied to the rest of the atoms.[40] Harmonic vibrational frequencies of Ac_2LKDADA, [V−H]$^-$, and [V+Ac_2LKDADA−H]$^-$ were calculated at the B3LYP/3-21G level of theory. Calculated vibrational frequencies of the model systems were used to obtain ZPE corrections and utilized in the RRKM modeling of the experimental data. Binding energies were determined based on single-point energies of the model systems by simulating precursor complexes and their products and by including the ZPE correction.

Acknowledgements

The authors would like to thank Dr. Dunyou Wang for helpful suggestions regarding the electronic structure calculations. This study was supported by the grant from the Separations and Analysis Program of the Chemical Sciences Division, Office of Basic Energy Sciences of the US Department of Energy (DOE). The research described in this manuscript was performed at the W. R. Wiley Environmental Molecular Sciences Laboratory (EMSL), a national scientific user facility sponsored by the DOE's Office of Biological and Environmental Research located at the Pacific Northwest National Laboratory (PNNL). PNNL is operated by Battelle for the U.S. Department of Energy. Theoretical calculations described in this work were performed by using the Molecular Science Computing Facility (MSCF) at EMSL and NWChem Version 5.1, developed and distributed by PNNL.

[1] P. A. Kollman, *Acc. Chem. Res.* **1977**, *10*, 365–371.
[2] D. Philp, J. F. Stoddart, *Angew. Chem.* **1996**, *108*, 1242–1286; *Angew. Chem. Int. Ed.* **1996**, *35*, 1155–1196.
[3] D. H. Williams, E. Stephens, D. P. O'Brien, M. Zhou, *Angew. Chem.* **2004**, *116*, 6760–6782; *Angew. Chem. Int. Ed.* **2004**, *43*, 6596–6616.
[4] J. Völker, K. J. Breslauer, *Annu. Rev. Biophys. Biomol. Struct.* **2005**, *34*, 21–42.
[5] T. Wyttenbach, M. T. Bowers, *Annu. Rev. Phys. Chem.* **2007**, *58*, 511–533.
[6] R. C. Dunbar, *Mass Spectrom. Rev.* **2004**, *23*, 127–158; R. C. Dunbar in *Principles of Mass Spectrometry Applied to Biomolecules* (Eds.: J. Laskin, C. Lifshitz), Wiley, New York, **2006**.
[7] P. D. Schnier, J. S. Klassen, E. F. Strittmatter, E. R. Williams, *J. Am. Chem. Soc.* **1998**, *120*, 9605–9613.
[8] N. Felitsyn, E. N. Kitova, J. S. Klassen, *Anal. Chem.* **2001**, *73*, 4647.
[9] J. Laskin, J. H. Futrell, *J. Phys. Chem. A* **2003**, *107*, 5836–5839.
[10] J. Laskin in *Principles of Mass Spectrometry Applied to Biomolecules* (Eds.: J. Laskin, C. Lifshitz), Wiley, New York, **2006**.
[11] J. Laskin, M. Byrd, J. H. Futrell, *Int. J. Mass Spectrom.* **2000**, *195*, 285–302.
[12] J. Laskin, J. H. Futrell, *J. Phys. Chem. A* **2000**, *104*, 5484–5494.
[13] J. Laskin, *Eur. J. Mass Spectrom.* **2004**, *10*, 259–267.
[14] J. Laskin, E. Denisov, J. H. Futrell, *J. Am. Chem. Soc.* **2000**, *122*, 9703–9714.
[15] Z. Yang, C. Lam, I. K. Chu, J. Laskin, *J. Phys. Chem. B* **2008**, *112*, 12468–12478.
[16] V. N. Nemykin, J. Laskin, P. Basu, *J. Am. Chem. Soc.* **2004**, *126*, 8604–8605.
[17] J. Laskin, Z. Yang, C. Lam, I. K. Chu, *Anal. Chem.* **2007**, *79*, 6607–6614.
[18] J. Laskin, Z. Yang, I. K. Chu, *J. Am. Chem. Soc.* **2008**, *130*, 3218–3230.
[19] Z. Yang, E. Vorpagel, J. Laskin, *J. Am. Chem. Soc.* **2008**, *130*, 13013–13022.
[20] a) A. N. Chatterjee, H. R. Perkins, *Biochem. Biophys. Res. Commun.* **1996**, *229*, 590–595; b) H. R. Perkins, *Biochem. J.* **1969**, *111*, 195–205; c) M. Nieto, H. R. Perkins, *Biochem. J.* **1971**, *123*, 773–787.
[21] H.-K. Lim, Y. Hsieh, B. Ganem, J. Henion, *J. Mass. Spectrom.* **1995**, *30*, 708–714.
[22] D. H. Williams, B. Bardsley, *Angew. Chem.* **1999**, *111*, 1264–1286; *Angew. Chem. Int. Ed.* **1999**, *38*, 1173–1193.
[23] a) T. J. D. Jørgensen, T. Staroske, P. Roepstorff, D. H. Williams, A. J. R. Heck, *J. Chem. Soc. Perkin Trans. 2* **1999**, 1859–1863; b) P. J. Vollmerhaus, E. Breukink, A. J. R. Heck, *Chem. Eur. J.* **2003**, *9*, 1556–1565; c) A. J. R. Heck, T. J. D. Jorgensen, *Int. J. Mass Spectrom.* **2004**, *236*, 11–23.
[24] a) P. J. Loll, P. H. Axelsen, *Annu. Rev. Biophys. Biomol. Struct.* **2000**, *29*, 265–289; b) S. Jusuf, P. J. Loll, P. H. Axelsen, *J. Am. Chem. Soc.* **2003**, *125*, 3988–3994.
[25] a) J. G. Lee, C. Sagui, C. Roland, *J. Am. Chem. Soc.* **2004**, *126*, 8384–8385; b) J. G. Lee, C. Sagui, C. Roland, *J. Phys. Chem. B* **2005**, *109*, 20588–20596.
[26] C. S. Hoaglund-Hyzer, A. E. Counterman, D. E. Clemmer, *Chem. Rev.* **1999**, *99*, 3037–3079.
[27] M. F. Jarrold, *Annu. Rev. Phys. Chem.* **2000**, *51*, 179–207.
[28] K. Breuker in *Principles of Mass Spectrometry Applied to Biomolecules* (Eds.: J. Laskin, C. Lifshitz), Wiley, New York, **2006**.
[29] R. A. Jockusch, P. D. Schnier, W. D. Price, E. F. Strittmatter, P. A. Demirev, E. R. Williams, *Anal. Chem.* **1997**, *69*, 1119–1126.
[30] a) T. J. D. Jørgensen, D. Delforge, J. Remacle, G. Bojesen, P. Roepstorff, *Int. J. Mass Spectrom.* **1999**, *188*, 63–85; b) T. J. D. Jørgensen, P. Hvelplund, J. U. Andersen, P. Roepstorff, *Int. J. Mass Spectrom.* **2002**, *219*, 659–670.
[31] a) D. H. Williams, M. P. Williamson, D. W. Butcher, S. J. Hammond, *J. Am. Chem. Soc.* **1983**, *105*, 1332–1339; b) R. K. Kannan, C. M. Harris, T. M. Harris, J. P. Waltho, N. J. Skelton, D. H. Williams, *J. Am. Chem. Soc.* **1988**, *110*, 2946–2953.
[32] J. Maple, U. Dinur, A. T. Hagler, *Proc. Natl. Acad. Sci. USA* **1988**, *85*, 5350–5354.
[33] J. Laskin, E. V. Denisov, A. K. Shukla, S. E. Barlow, J. H. Futrell, *Anal. Chem.* **2002**, *74*, 3255–3261.
[34] S. A. Schaffer, K. Q. Tang, G. A. Anderson, D. C. Prior, H. R. Udseth, R. D. Smith, *Rapid Commun. Mass Spectrom.* **1997**, *11*, 1813–1817.

[35] M. W. Senko, J. D. Canterbury, S. Guan, A. G. Marshall, *Rapid Commun. Mass Spectrom.* **1996**, *10*, 1839–1844.
[36] a) http://www.rcsb.org, and PDB code is 1aa5; b) P. J. Loll, A. E. Bevivino, B. D. Korty, P. H. Axelen, *J. Am. Chem. Soc.* **1997**, *119*, 1516–1522.
[37] M. J. D. Powell, *Math. Program.* **1977**, *12*, 241–254.
[38] E. J. Bylaska, W. A. de Jong, N. Govind, K. Kowalski, T. P. Straatsma, M. Valiev, D. Wang, E. Apra, T. L. Windus, J. Hammond, P. Nichols, S. Hirata, M. T. Hackler, Y. Zhao, P.-D. Fan, R. J. Harrison, M. Dupuis, D. M. A. Smith, J. Nieplocha, V. Tipparaju, M. Krishnan, Q. Wu, T. Van Voorhis, A. A. Auer, M. Nooijen, E. Brown, G. Cisneros, G. I. Fann, H. Fruchtl, J. Garza, K. Hirao, R. Kendall, J. A. Nichols, K. Tsemekhman, K. Wolinski, J. Anchell, D. Bernholdt, P. Borowski, T. Clark, D. Clerc, H. Dachsel, M. Deegan, K. Dyall, D. Elwood, E. Glendening, M. Gutowski, A. Hess, J. Jaffe, B. Johnson, J. Ju, R. Kobayashi, R. Kutteh, Z. Lin, R. Littlefield, X. Long, B. Meng, T. Nakajima, S. Niu, L. Pollack, M. Rosing, G. Sandrone, M. Stave, H. Taylor, G. Thomas, J. van Lenthe, A. Wong, and Z. Zhang, NWChem, A Computational Chemistry Package for Parallel Computers, Version 5.1, Pacific Northwest National Laboratory, Richland, WA (USA), **2007**.
[39] G. Black, J. Daily, B. Didier, T. Elsethagen, D. Feller, D. Gracio, M. Hackler, S. Havre, D. Jones, E. Jurrus, T. Keller, C. Lansing, S. Matsumoto, B. Palmer, M. Peterson, K. Schuchardt, E. Stephan, L. Sun, K. Swanson, H. Taylor, G. Thomas, E. Vorpagel, T. Windus, C. Winters, ECCE, A Problem Solving Environment for Computational Chemistry, Software Version 4.5.1, Pacific Northwest National Laboratory, Richland, WA (USA), **2007**.
[40] The levels of theory applied to different atoms in ONIOM calculations of the structures of $[V-H]^-$ and $[V+Ac_2LKDADA-H]^-$ are detailed in the Supporting Information.

Received: September 30, 2008
Published online: January 20, 2009

